Sequence of events during the last deglaciation in Southern Ocean sediments and Antarctic ice cores

A. Shemesh, D. Hodell, X. Crosta, S. Kanfoush, C. Charles, T. Guilderson

Sequence of events during the last deglaciation in Southern Ocean sediments and Antarctic ice cores

A. Shemesh,[1] D. Hodell,[2] X. Crosta,[1] S. Kanfoush,[2,3] C. Charles,[4] and T. Guilderson[5]

Received 17 October 2000; revised 27 March 2002; accepted 27 March 2002; published 15 October 2002.

[1] The last glacial to interglacial transition was studied using down core records of stable isotopes in diatoms and foraminifera as well as surface water temperature, sea ice extent, and ice-rafted debris (IRD) concentrations from a piston core retrieved from the Atlantic sector of the Southern Ocean. Sea ice is the first variable to change during the last deglaciation, followed by nutrient proxies and sea surface temperature. This sequence of events is independent of the age model adopted for the core. The comparison of the marine records to Antarctic ice CO_2 variation depends on the age model as ^{14}C determinations cannot be obtained for the time interval of 29.5–14.5 ka. Assuming a constant sedimentation rate for this interval, our data suggest that sea ice and nutrient changes at about 19 ka B.P. lead the increase in atmospheric pCO_2 by approximately 2000 years. Our diatom-based sea ice record is in phase with the sodium record of the Vostok ice core, which is related to sea ice cover and similarly leads the increase in atmospheric CO_2. If gas exchange played a major role in determining glacial to interglacial CO_2 variations, then a delay mechanism of a few thousand years is needed to explain the observed sequence of events. Otherwise, the main cause of atmospheric pCO_2 change must be sought elsewhere, rather than in the Southern Ocean. *INDEX TERMS:* 3344 Meteorology and Atmospheric Dynamics: Paleoclimatology; 4267 Oceanography: General: Paleoceanography; 4845 Oceanography: Biological and Chemical: Nutrients and nutrient cycling; 4870 Oceanography: Biological and Chemical: Stable isotopes; 9325 Information Related to Geographic Region: Atlantic Ocean; *KEYWORDS:* biogenic opal, stable isotopes, diatoms, IRD, last glacial, Southern Ocean

Citation: Shemesh, A., D. Hodell, X. Crosta, S. Kanfoush, C. Charles, and T. Guilderson, Sequence of events during the last deglaciation in Southern Ocean sediments and Antarctic ice cores, *Paleoceanography*, *17*(4), 1056, doi:10.1029/2000PA000599, 2002.

1. Introduction

[2] Understanding glacial-to-interglacial atmospheric CO_2 variations requires a coupled ocean-atmosphere approach where ice core data are integrated with marine sediment records. Recent studies indicate that the most promising scenarios for explaining glacial-to-interglacial CO_2 change are tied to sea surface conditions, such as sea ice extent, gas exchange, and nutrient cycling in the Southern Ocean [*Broecker*, 1982; *Elderfield and Rickaby*, 2000; *Francois et al.*, 1997; *Stephens and Keeling*, 2000; *Toggweiler*, 1999]. The phasing of proxy indicators at terminations [*Broecker and Henderson*, 1998; *Labracherie et al.*, 1989] in marine and polar ice core records provide clues about the mechanisms controlling climate fluctuations. Here we focus on the last deglaciation (Termination I) as recorded in a 13.7-m piston core (TN057-13-PC4) retrieved from 53.2°S, 5.1°E in the Atlantic sector of the Southern Ocean, south of the present day Polar front. Chronological control for the core is provided by AMS ^{14}C dates on monospecific samples of the plantonic foraminifera *Neogloboquadrina pachyderma* (Table 1), which results in the best dated core in the Southern Ocean south of the Polar Front. The chronology for the last glaciation and the beginning of the deglaciation is based on linear interpolation between two AMS ^{14}C dates at 14.5 and 29.5 ka. Additional dates for this period cannot be obtained because of the low abundance of foraminifera. Therefore we tested our age model by comparing IRD abundances between cores TN057-13-PC4 and TN057-21 (located at 41°S in the subantarctic Atlantic region). The chronology of TN057-21 is well established by correlation to the extensively ^{14}C-dated core RC11-83 [*Charles et al.*, 1996; *Ninnemann et al.*, 1999]. Prominent IRD peaks resulting from ice sheet instability have been shown to be synchronous across the South Atlantic [*Kanfoush et al.*, 2000]. Aligning IRD peaks of both cores results in insignificant changes to our chronology, which is derived by assuming a constant sedimentation rate between the two AMS ^{14}C dates at 14.5 and 29.5 ka. Sedimentation rates average ~10 cm/kyr between 29.5 and 14.5 ka during the last glaciation and increase to ~48 cm/ka during the period of deglaciation and the Holocene. The change in sedimentation rate coincides with an increase in biogenic silica content. All data are presented on a ^{14}C age model that have

[1]Department of Environmental Sciences and Energy Research, Weizmann Institute of Science, Rehovot, Israel.
[2]Department of Geological Sciences, University of Florida, Gainesville, Florida, USA.
[3]Now at Department of Geology, Utica College of Syracuse University, Utica, New York, USA.
[4]Scripps Institution of Oceanography, University of California, San Diego, La Jolla, California, USA.
[5]Lawrence Livermore National Laboratory, Livermore, California, USA.

0883-8305/02/2000PA000599$12.00

Table 1. Age-Depth Relation in Core TTN057-13-PC4

Sample	Depth, cm	Conventional ^{14}C, years	Error, years	Calibrated Age, years	Reference
X 18–23	20	1590	±80	720	*Stuiver et al.* [1998]
X 63–65	63	2630	±60	1830	*Stuiver et al.* [1998]
VIII 21–26	256	6850	±60	6930	*Stuiver et al.* [1998]
VII 63–68	449	9340	±60	9480–9590	*Stuiver et al.* [1998]
VII 87–92	473	9370	±80	9600	*Stuiver et al.* [1998]
VI 0–5	536	10,050	±40	10,310	*Stuiver et al.* [1998]
VI 12–17	548	9970	±90	10,290	*Stuiver et al.* [1998]
V 60–62	741	13,140	±50	14,400, 14,550	*Bard et al.* [1998]
V 81–86	763	13070	±80	14,320, 14,470	*Bard et al.* [1998]
IV 90–92	919	26,360	±150	29,130, 29,980	*Bard et al.* [1998]
IV 90–92repl.	919	26,360	±150	29,130, 29,980	*Bard et al.* [1998]
IV 141–143	970	33,420	±250	36,990, 37,830	*Bard et al.* [1998]
II 50–52	1180	53,720	±3600	-	-
II 50–52repl.	1180	52,060	±2200	-	-
I 50–67	1289	>42,560	-	-	-

been converted to calendar years [*Bard et al.*, 1998; *Stuiver et al.*, 1998] with a 800-year reservoir effect [*Kanfoush et al.*, 2000]. The records are compared with the Vostok and Byrd ice cores using the timescale of Blunier [*Blunier et al.*, 1998] that facilitates comparison between Northern and Southern Hemisphere records.

2. Results and Discussion

[3] Multiple proxies were analyzed in the same samples from TN057-13 including geochemical, floral, faunal and sedimentological parameters to elucidate sea surface physical, chemical and nutrient availability characteristics (Figure 1). Isotope analyses included oxygen isotopes of planktic foraminifera (*Neogloboquadrina pachyderma* sinistral) and of diatom biogenic silica as proxies of surface water temperature and salinity, and carbon and nitrogen isotopes of diatom-intrinsic organic matter as proxies of nutrient cycling. Diatom assemblages were examined quantitatively to estimate sea ice cover and February SST. Concentrations of ice-rafted detritus (IRD) were calculated by counting a minimum of 500 grains in the 150 μm to 2 mm size fraction [*Kanfoush et al.*, 2000].

[4] The sediment consists mainly of diatoms, reaching about 85% opal during the Holocene and 50% during the glacial stage, and a mixture of clays and IRD. The diatom flora is dominated throughout the core by an open ocean assemblage (mainly *Fragilariopsis kerguelensis* and *Thalassiosira lentiginosa*), varying between 90% during the Holocene and 60% during the last glacial. Diatom-assemblages do not change markedly across Termination I, and therefore the isotope signals (^{18}O, ^{13}C, and ^{15}N) of biogenic silica are free from vital effects [*Hinga et al.*, 1994; *Popp et al.*, 1998; *Sigman et al.*, 1999] and represent surface water characteristics. Diatom estimates of February sea surface temperatures [*Crosta et al.*, 1998] show that the difference between the last glacial and Holocene is about 2–3°C over Termination I. The average from 35 to 20 ka was 2.2°C and increased to an average of 4.2°C between 15 and 6 ka (Figure 1f). However, the fine structure of the curve indicates two minima at 13 and 11 ka, synchronous with the Antarctic Cold Reversal (ACR [*Jouzel et al.*, 1995; *Sowers and Bender*, 1995]) and another smaller cooling event in the Byrd oxygen isotope record [*Fischer et al.*, 1999]. Maximum temperature of 6°C occurs at ~10 ka and exceeds average glacial values by 4°C. The subsequent early Holocene cooling is in accord with other South Atlantic temperature records [*Zielinski et al.*, 1998]. The February SST record shows (Figure 1f) that full warming is completed in 10 ka starting at 20 ka B.P.

[5] δ^{18}Osi depends on the temperature and the isotopic composition of seawater (δ^{18}Ow) from which it was deposited [*Juillet-Leclerc and Labeyrie*, 1987; *Shemesh et al.*, 1992]. The latter changes as a function of the amount of isotopically light water delivered when icebergs melt. The minima in $\delta^{18}O_{si}$ correspond with cooling events or constant surface temperature as indicated independently by the diatom transfer functions (Figure 1f). Because decreased temperature should lead to increased δ^{18}O silica, minima in δ^{18}O silica must represent reduced δ^{18}O of seawater resulting from meltwater influx to surface waters [*Francois et al.*, 1997; *Labeyrie et al.*, 1986; *Shemesh et al.*, 1994]. The isotopic depletion of diatom opal ^{18}O ($\delta^{18}O_{si}$; Figure 1b) during the last glaciation is consistent with other Southern Ocean cores [*Shemesh et al.*, 1994, 1992, 1993].

[6] In contrast to the glacial δ^{18}O diatom signal, δ^{18}O of *N. pachyderma* (Figure 1a) shows the most enriched values during the glacial (~5‰) which then decrease to an average of 3.7‰ in the early Holocene. The low abundance of *N. pachyderma* during the glacial and the fact that it doesn't record the full glacial-to-interglacial δ^{18}O amplitude suggests that it may have been environmentally excluded from the surface during times of meltwater stratification when it resided at deeper depths. Using the radiocarbon age model of the marine core and the Blunier timescale for Vostok and Byrd [*Blunier et al.*, 1998], the two oxygen isotope records from TTN057-13 are well correlated to the δD of Vostok (Figure 2) and δ^{18}O record at Byrd during Termination I. Both diatom and *N. pachyderma* δ^{18}O capture the ACR, and the marine isotopic records are synchronous with the ice core records when both plotted on their independent timescales. The ACR at 14 ka and a small reversal at 11 ka in

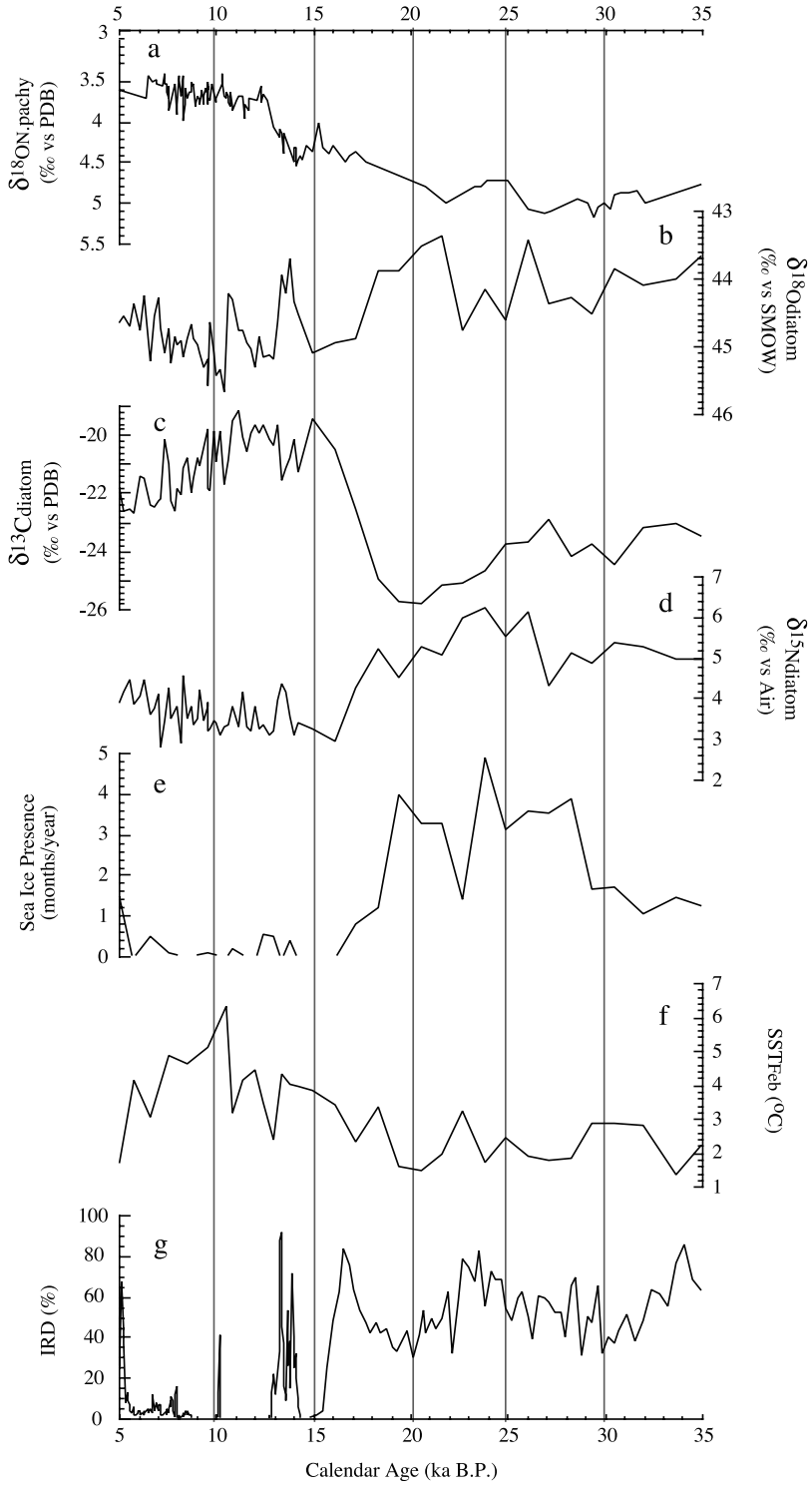

Figure 1. Down core records of (a) $\delta^{18}O_{pachy}$, (b) $\delta^{18}O_{si}$, (c) $\delta^{13}C_{diatom}$, (d) $\delta^{15}N_{diatom}$, (e) sea ice presence, (f) February sea surface temperature, and (g) ice-rafted debris [*Kanfoush et al.*, 2000] in core TTN057-13. Chronological control for the core is provided by 15 AMS ^{14}C dates on monospecific samples of the foraminifera *Neogloboquadrina pachyderma* from 13 stratigraphic horizons to a depth of 11.8 meters (Table 1). Average standard deviation (SD) is indicated for each parameter.

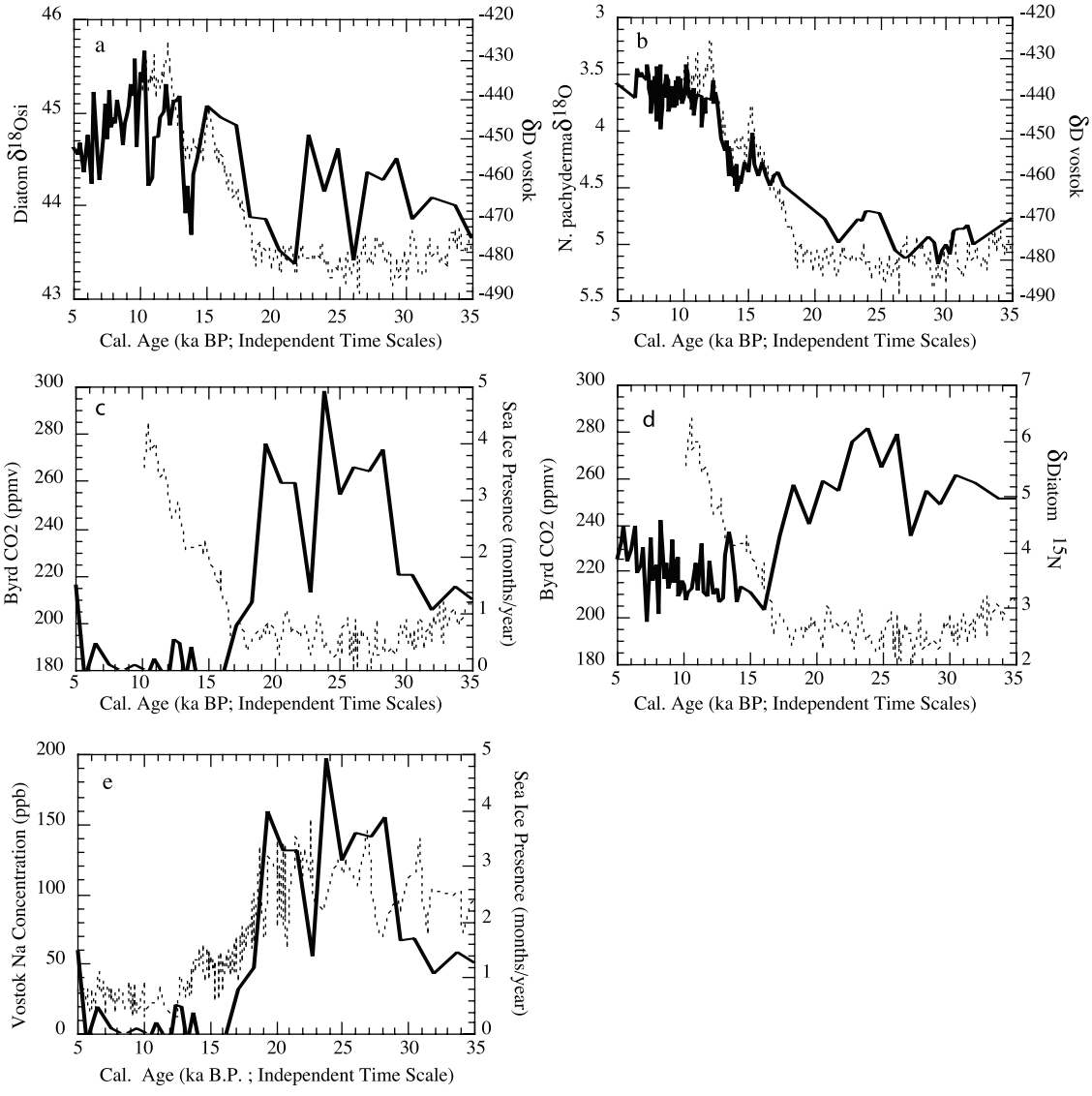

Figure 2. Comparison of TTN057-13 diatom (a) $\delta^{18}O_{si}$ and (b) $\delta^{18}O_{pachy}$ with Vostok δD record (dashed line). The ACR is captured by both the diatom and the foraminifera ^{18}O signals. Byrd CO_2 record (dashed line) compared with (c) TTN057-13 sea ice presence record and (d) $\delta^{15}N_{diatom}$. The ice core records [*Blunier et al.*, 1998] and the marine records are on independent timescales for all panels. (e) Vostok Na record [*Petit et al.*, 1999] compared with sea ice presence in core TTNO57-13.

Byrd correspond to two meltwater spikes in the $\delta^{18}O_{si}$ curve and SST cooling.

[7] IRD concentrations during the last glacial are generally higher than during the Holocene (Figure 1g). The major meltwater pulses are associated with high IRD, including the ACR event. During the ACR, the IRD is composed of both quartz and ash, suggesting deposition by melting of tabular icebergs calved from the Antarctic continent. The synchroneity of meltwater, IRD and surface temperature during the ACR may point to instability of the Antarctic Ice Sheet as the cause of this event [*Kanfoush et al.*, 2000].

[8] Higher relative abundance of sea ice diatoms (10–15%; mainly *F. curta* and *F. obliquecostata*) argue for an enhanced sea ice cover during the last glacial at this site. The glacial sea ice assemblage decreases rapidly to modern values (0–2%) in about 1000 years, from 19 ka to 18 ka. The diatom transfer function indicates that ice persisted for 4 to 5 months per year during the last glacial and for less than one month after 18 ka (Figure 1e). Petit et al. [*Petit et al.*, 1999] suggested that the variation of sodium concentrations in the Vostok ice core is related to sea ice cover and the vigor of atmospheric circulation. Indeed, the diatom based sea ice estimate from TN057-13 is similar to the Na record of Vostok, with each record on their independent timescale (Figure 2e). This observation supports both the suggested relationship between sea ice and Na, and our temporal comparison between the marine sediment core and Vostok record.

[9] The $\delta^{13}C$ and $\delta^{15}N$ of diatom-intrinsic organic matter (Figure 1c and 1d, respectively) generally follow the well-

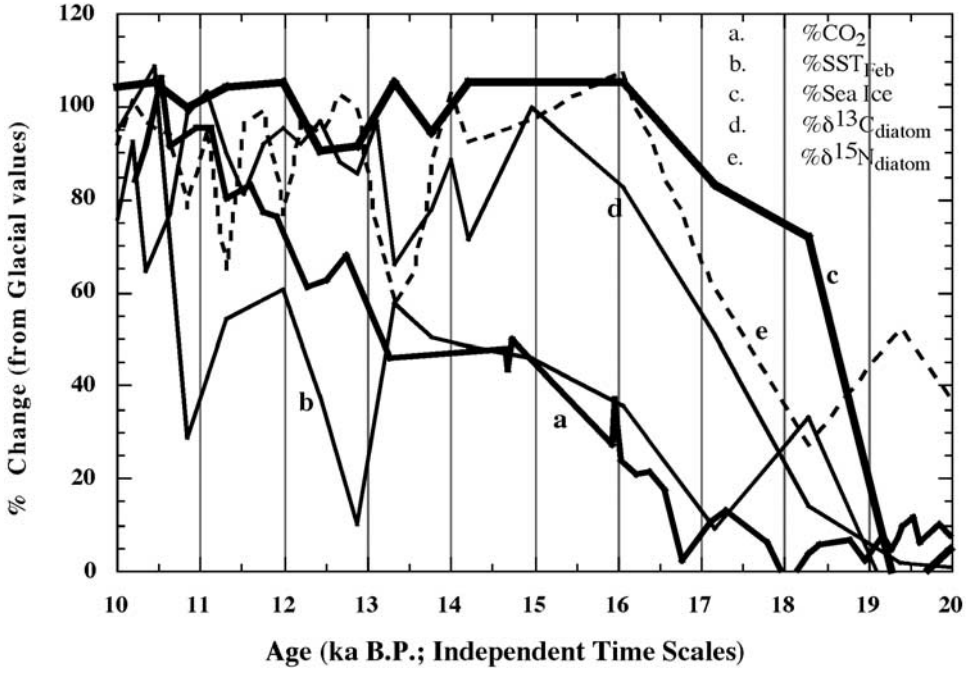

Figure 3. Normalized curves representing the change between average glacial values and Holocene values of Byrd CO_2 and TTN057-13 SST, sea ice presence, $\delta^{13}C_{diatom}$, and $\delta^{15}N_{diatom}$. Timescale of TTN057-13 is independent of the ice core record.

known patterns of increasing $\delta^{15}N$ and decreasing $\delta^{13}C$ in sediments south of the Polar Front [*Bentaleb and Fontugne*, 1998; *Francois et al.*, 1997; *Rosenthal et al.*, 2000; *Singer and Shemesh*, 1995]. However, during times of extensive sea ice cover (e.g., 27 to 20 ka), both $\delta^{13}C_{diatom}$ and $\delta^{15}N_{diatom}$ decrease simultaneously to a minimum at 20 ka. When sea ice starts to diminish, $\delta^{15}N_{diatom}$ is further depleted while $\delta^{13}C_{diatom}$ is enriched to its Holocene values to create the general pattern of anti-correlation.

[10] The nitrogen isotope signal indicates higher relative utilization of dissolved nitrate in the nutrient pool [*Altabet and Francois*, 1994] during the last glacial when $\delta^{18}O_{si}$ indicates maximum water column stratification due to melt water input. Sea ice extent is also at its maximum at this time and seasonal melting may also increase surface water stratification. The shift towards lower $\delta^{15}N_{diatom}$ values during the Holocene indicates lower NO_3 utilization and occurs synchronously with diminishing sea ice and reduced meltwater presence as deduced by diatom assemblages and $\delta^{18}O_{si}$, respectively.

[11] Nitrogen and carbon isotopes of diatom-intrinsic organic matter are generally anti-correlated during Termination I and the Holocene. Between 26 ka and the LGM at 20 ka, however, both $\delta^{15}N_{diatom}$ and $\delta^{13}C_{diatom}$ show a depletion that can be interpreted as decreasing primary production (lower nutrient utilization) due to inhibition by sea ice cover [*Burckle*, 1984; *Gersonde and Wefer*, 1987]. We rule out increasing the nutrient content of surface waters through deep mixing as an explanation because $\delta^{18}O_{si}$ indicates meltwater input at this site and the consequent increase in stratification of surface waters during the last glaciation [*Francois et al.*, 1997] argues against enhanced deep mixing. Vital effects are not likely to dominate the signals of $\delta^{15}N_{diatom}$ and $\delta^{13}C_{diatom}$ organic matter as the diatom assemblages and shape are almost identical during the LGM and Holocene and only minor changes in species composition are observed [*Hinga et al.*, 1994; *Popp et al.*, 1998]. Beginning at 19 ka, $\delta^{13}C_{diatom}$ increases rapidly while $\delta^{15}N_{diatom}$ continues to decrease during the last deglaciation. At the same time, biogenic silica content and accumulation rates increase indicating increased productivity in the absence of sea ice. Dissolution can not account for these changes as the preservation index is almost constant during this period. This productivity increase overcomes the predicted decrease in $\delta^{13}C_{diatom}$ due to increasing atmospheric CO_2 at this time and is reflected in the 5.7‰ enrichment in $\delta^{13}C_{diatom}$. This productivity increase is not reflected in the nitrogen isotopes. On the contrary, $\delta^{15}N_{diatom}$ drops to lower values indicating lower nitrate utilization. The way to reconcile these observations is by increased productivity associated with increased upwelling of deep water (high in TCO_2 and NO_3) that generates a situation in which the carbon demand exceeds the nitrogen demand. It is probably the first step in developing the present day situation, where the region is characterized by High-Nutrient, Low-Chlorophyll [*Martin*, 1990] surface waters in which NO_3 is no longer a limiting nutrient. Independent support for this scenario is provided by the increase in $\delta^{13}C_{pachy}$ during Termination I, pointing to increasing productivity.

[12] Because all proxies were measured in the same core, the relative timing of changes among variables holds regardless of the absolute timescale adopted for the core. TNO57-13-PC4 is the best dated core available south of the Polar Front for comparison with polar ice records. We

obtained the same leads and lags between the marine proxies and δD and CO_2 records during the last deglaciation using several alternative age models for the Vostok ice core [*Blunier et al.*, 1998; *Jouzel et al.*, 1995; *Sowers and Bender*, 1995]. In Marine Stage 3, the Sowers' timescale [*Sowers and Bender*, 1995] yields better agreement with $\delta^{18}O_{si}$, but we retain the Blunier's timescale [*Blunier et al.*, 1998] because it provides a mechanism for comparison between Antarctic and Greenland ice cores.

[13] Comparison of diatom sea ice, $\delta^{15}N_{diatom}$ and $\delta^{13}C_{diatom}$ in TTN057-13 with Byrd CO_2, each on their independent timescales (Figures 2 and 3), reveals that atmospheric CO_2 starts to increase when sea ice coverage diminishes to its lowest extent at 17 ka B.P. (Figure 2c). $\delta^{15}N_{diatom}$ leads the change in CO_2 by 7 ka starting at 24 ka and $\delta^{13}C_{diatom}$ leads CO_2 by 2 ka starting at 19 ka B.P. The time required for each tracer to change from its glacial values to full Holocene values is 3 ka for sea ice, 8 ka for $\delta^{15}N_{diatom}$, 4 ka for $\delta^{13}C_{diatom}$, and 7 ka for pCO_2. In contrast to the sea ice, $\delta^{13}C_{diatom}$ and $\delta^{15}N_{diatom}$ signals, which lead CO_2, Feb. SST and $\delta^{13}C_{pachy}$, increases at the same time as pCO_2.

[14] We focus on the sequence of events during Termination I (Figure 3) by expressing the change in each variable as a percentage of the maximum values reached during the early Holocene. The marine records show that sea ice leads $\delta^{15}N_{diatom}$, and $\delta^{13}C_{diatom}$ (Figure 3). The TNO57-13-PC4 record indicates that this lead is on the order of 1500 years. Whereas the difference in timing among sea ice, nitrogen and carbon isotopes is relatively small, with each reaching their maximum Termination values at ~16 ka, temperature starts to rise only 2 ka after these parameters and at a much slower pace. If the Byrd CO_2 record on the Blunier timescale is representative of atmospheric pCO_2 rise, then sea ice and nutrient cycling changes lead atmospheric pCO_2 by 2 ka.

[15] Recently, analysis of satellite ocean color, sea surface temperature and sea ice cover in the Southern Ocean indicate a strong coupling between biological activity and sea ice duration. Both parameters act in concert to affect present day gas exchange, and may have had an important role in determining glacial to interglacial variation of atmospheric CO_2 [*Moore et al.*, 2000]. In the same vein, model calculations show that extended sea ice duration and melt water stratification in the Southern Ocean during the LGM were responsible for a 67ppm lowering of atmospheric CO_2 concentrations [*Stephens and Keeling*, 2000]. Our data provide the first down core record to test these hypotheses. Indeed, a close relation between sea ice extent and nutrient cycling is observed, suggesting that sea ice may have affected the biological activity of the surface water. However, the nutrient indicators as well as sea ice extent significantly lead atmospheric pCO_2 and reach their maximum before CO_2 starts to rise. Assuming that the Na record is correlated to sea ice extent, this phase relationship is supported by the 2.7 ka lead of Na decrease over increasing pCO_2 in Vostok and Byrd. If the Southern Ocean plays a major role in determining glacial to interglacial atmospheric CO_2 variations, either by gas exchange or by the biological pump, one would expect a better match between the timing and magnitude of their responses. The observed lead of sea ice extent indicates that this parameter may be the trigger to biological activity and gas exchange variations. However, as gas exchange is a rapid process, an immediate response of glacial to interglacial atmospheric CO_2 changes to sea ice variations would be expected. We conclude that delayed mechanism(s), on the order of a few thousand years, must be invoked to explain the observed sequence of events. Taking into account that the patterns measured in TN057-13 are common to other sectors of the Southern Ocean [*Crosta et al.*, 1998; *Francois et al.*, 1997; *Ninnemann et al.*, 1999; *Rosenthal et al.*, 2000], and that the Southern Ocean is longitudinally homogeneous, it is reasonable to consider the Atlantic sector as representative of the region south of the Polar Front. Hence, in the absence of a mechanism that explains delayed CO_2 response to sea ice and nutrient cycling in the Southern Ocean, the dominant control of glacial to interglacial pCO_2 variation must be sought elsewhere.

References

Altabet, M. A., and R. Francois, Sedimentary nitrogen isotopic ratio as a recorder for surface ocean nitrate utilization, *Global Biogeochem. Cycles*, *8*(1), 103–116, 1994.

Bard, E., M. Arnold, B. Hamelin, N. Tisnerat-Laborde, and G. Cabioch, Radiocarbon calibration by means of mass spectrometric Th-230/U-234 and C-14 ages of corals: An updates database including samples from Barbados, Mururoa and Tahiti, *Radiocarbon*, *40*(3), 1085–1092, 1998.

Bentaleb, I., and M. Fontugne, The role of the southern Indian Ocean in the glacial to interglacial atmospheric CO_2 change: Organic carbon isotope evidences, *Global Planet. Change*, *16*, 25–36, 1998.

Blunier, T., et al., Asynchrony of Antarctic and Greenland climate change during the last glacial period, *Nature*, *394*, 739–743, 1998.

Broecker, W. S., Ocean chemistry during glacial time, *Geochim. Cosmochim. Acta*, *46*, 1689–1705, 1982.

Broecker, W. S., and G. M. Henderson, The sequence of events surrounding Termination II and their implications for the cause of glacial-interglacial CO_2 changes, *Paleoceanography*, *13*(4), 352–364, 1998.

Burckle, L. H., Diatom distribution and paleoceanographic reconstruction in the Southern Ocean—Present and Last Glacial Maximum, *Mar. Micropaleontol.*, *9*, 241–261, 1984.

Charles, C. D., J. Lynch-Stieglitz, U. S. Ninnemann, and R. G. Fairbanks, Climate connections between the hemispheres revealed by deep sea sediment core/ice core correlation, *Earth Planet. Sci. Lett.*, *142*, 19–27, 1996.

Crosta, X., J. J. Pichon, and L. H. Burckle, Application of modern analog technique to marine Antarctic diatoms: Reconstruction of the maximum sea ice extent at the Last Glacial Maximum, *Paleoceanography*, *13*(3), 284–297, 1998.

Elderfield, H., and R. E. M. Rickaby, Oceanic Cd/P ratio and nutrient utilization in the glacial Southern Ocean, *Nature*, *405*, 305–310, 2000.

Fischer, H., M. Wahlen, J. Smith, D. Mastroianni, and B. Deck, Ice core records of atmospheric CO_2 around the last three glacial terminations, *Science*, *283*, 1712–1714, 1999.

Francois, R., et al., Contribution of Southern Ocean surface-water stratification to low atmospheric CO_2 concentrations during the last glacial period, *Nature*, *389*, 929–935, 1997.

Gersonde, R., and G. Wefer, Sedimentation of biogenic siliceous particles in Antarctic waters from the Atlantic sector, *Mar. Micropaleontol.*, *11*, 311–332, 1987.

Hinga, K. R., M. A. Arthur, M. E. Q. Pilson, and D. Withaker, Carbon isotope fractionation by marine phytoplankton culture: The effects of CO_2 concentration, pH, temperature, and species, *Global Biogeochem. Cycles*, *8*(1), 91–102, 1994.

Jouzel, J., et al., The 2-step shape and timing of the last deglaciation in Antarctica, *Clim. Dyn.*, *11*, 151–161, 1995.

Juillet-Leclerc, A., and L. Labeyrie, Temperature dependence of the oxygen isotopic fractiona-

tion between diatom silica and water, *Earth Planet. Sci. Lett.*, *84*, 69–74, 1987.
Kanfoush, S. L., et al., Millennial-scale instability of the Antarctic ice sheet during the last glaciation, *Science*, *288*, 1815–1819, 2000.
Labeyrie, L. D., et al., Melting history of Antarctica during the past 60,000 years, *Nature*, 1986.
Labracherie, M., L. D. Labeyrie, and J. E. A. Duprat, The last deglaciation in the Southern Ocean, *Paleoceanography*, *4*, 629–638, 1989.
Martin, J., Glacial-interglacial CO_2 change: The iron hypothesis, *Paleoceanography*, *5*, 1–13, 1990.
Moore, J. K., M. R. Abbott, J. G. Richman, and D. M. Nelson, The Southern Ocean at the Last Glacial Maximum: A strong sink for atmospheric CO_2, *Global Biogeochem. Cycles*, *14*(1), 455–475, 2000.
Ninnemann, U. S., C. D. Charles, and D. A. Hodell, Origin of global millennial scale climate events: Constraints from the Southern Ocean deep sea sedimentary record, in *Mechanisms of Global Climate Change at Millennial Time Scales, Geophys. Monogr. Ser.*, vol. 112, edited by P. U. Clark, R. S. Webb, and L. D. Keigwin, pp. 99–112, AGU, Washington, D.C., 1999.
Petit, J. R., et al., Climate and atmospheric history of the past 420,000 years from the Vostok ice core, Antarctica, *Nature*, *399*, 429–436, 1999.
Popp, B. N., et al., Effect of phytoplankton cell geometry on carbon isotopic fractionation, *Geochim. Cosmochim. Acta*, *62*(1), 69–77, 1998.
Rosenthal, Y., M. Dahan, and A. Shemesh, The glacial Southern Ocean: A source of atmospheric CO_2 as inferred from carbon isotopes in diatoms, *Paleoceanography*, *15*(1), 65–75, 2000.
Shemesh, A., L. H. Burckle, and J. D. Hays, Meltwater input to the Southern Ocean during the Last Glacial Maximum, *Science*, *266*, 1542–1544, 1994.
Shemesh, A., C. D. Charles, and R. G. Fairbanks, Oxygen isotopes in biogenic silica: Global changes in ocean temperature and isotopic composition, *Science*, *256*, 1434–1436, 1992.
Shemesh, A., S. A. Macko, C. D. Charles, and G. H. Rau, Isotopic evidence for reduced productivity in the glacial Southern Ocean, *Science*, *262*, 407–410, 1993.
Sigman, D. M., M. A. Altabet, R. Francois, D. C. McCorkle, and J. F. Gaillard, The isotopic composition of diatom-bound nitrogen in the Southern Ocean sediments, *Paleoceanography*, *14*(2), 118–134, 1999.
Singer, A. J., and A. Shemesh, Climatically linked carbon isotope variation during the past 430,000 years in Southern Ocean sediments, *Paleoceanography*, *10*(2), 171–177, 1995.
Sowers, T., and M. Bender, Climate records covering the last deglaciation, *Science*, *269*, 210–214, 1995.
Stephens, B. B., and R. F. Keeling, The influence of Antarctic sea ice on glacial-interglacial CO_2 variations, *Nature*, *404*, 171–174, 2000.
Stuiver, M., P. J. Reimer, and T. F. Braziunas, High-precision radiocarbon age calibration for terrestrial and marine samples, *Radiocarbon*, *40*(3), 1127–1151, 1998.
Toggweiler, J. R., Variation of atmospheric CO_2 by ventilation of the ocean's deepest water, *Paleoceanography*, *14*(5), 571–588, 1999.
Zielinski, U., R. Gersonde, R. Sieger, and D. Futterer, Quaternary surface water temperature estimations: Calibration of diatom transfer function for the Southern Ocean, *Paleoceanography*, *13*(4), 365–383, 1998.

C. Charles, Scripps Institution of Oceanography, University of California, San Diego, La Jolla, CA 92093, USA.
X. Crosta and A. Shemesh, Department of Environmental Sciences and Energy Research, Weizmann Institute of Science, Rehovot 76100, Israel. (aldo.shemesh@weizmann.ac.il)
T. Guilderson, Lawrence Livermore National Laboratory, Livermore, CA 94550, USA.
D. Hodell, Department of Geological Sciences, University of Florida, Gainesville, FL 32611–2120, USA.
S. Kanfoush, Department of Geology, Utica College of Syracuse University, Utica, NY 13502, USA.